한국전산구조공학회
1999년도 가을학술발표회 논문집

다층 반무한 지반-구조물계의 입사파 응답해석

3D Incident Wave Response of Structures on Layered Media

김문겸* 조우연** 고재필***
Kim, Moon Kyum Cho, Woo Yeon Koh, Jae Pil

ABSTRACT

Dynamic interaction analysis of surface structure on layered half-space is performed in frequency domain under incident wave excitation. This present study adopts a coupling method that combines the finite element(FE) for the flexible structures and boundary element(BE) for the layered half-space. A semi-analytical approach is employed to reduce the integration range of wavenumbers in the BE formula. For the incident wave input, the response is decomposed and formulated after the impedance matrix for the structure system. Numerical examples are presented to demonstrate the accuracy of the method. The examples show the feasibility of an extended application to the complicated dynamic analysis of structures on layered media under incident wave excitation.

1. INTRODUCTION

The dynamic interaction is an important factor when considering soil-structure systems under incident wave excitation. A number of methods were introduced during the past decades to solve this mixed boundary value problem in the frequency domain. Wong and Luco(1986) developed the semi-analytical method, Mohammadi and Karabalis(1995), Qian et al.(1996) used numerical finite element and boundary element techniques. However, its formulation is complicated in use and the soil media is limited to a homogeneous one.

In this study, dynamic interaction analysis on layered half-space is performed under incident wave excitation. The coupling method that combines FE for the structures and BE for layered half-space makes it feasible. Regarding the layered half-space, Green's functions are adopted in terms of displacements for dynamic point loads determined by expanding the two-dimensional fundamental solutions by Kim et al.(1999) to three-dimensional fundamental solutions. For the incident wave input, the response is decomposed into the response due to external and inertial forces, and the surface input motion. Both forces can be easily formulated

* 연세대학교 토목공학과 교수, 정회원
** 연세대학교 토목공학과 박사과정
*** 한국가스공사 연구개발원 연구원

after the impedance matrix for the structure system and the control ground motions are decided. In order to verify the fundamental solutions, response of rigid circular structure is tested. Then the incident wave response of flexible circular structure resting on the layered half-space is examined to demonstrate the capability of the developed procedure.

2. BOUNDARY ELEMENT FORMULATION

As shown in *Figure* 1, when the finite portion of half-space is occupied by the foundation, the equilibrium conditions and the compatibility conditions for the displacements are imposed over the entire surface Γ, the horizontally layered half-space is recreated. The representation applied to the surface Γ is reduced to

$$u_i(\boldsymbol{x}) = \int_\Gamma u_{ji}^*(\boldsymbol{x}_s;\boldsymbol{x}) t_j(\boldsymbol{x}) d\Gamma \qquad (i,j = x,y,z) \tag{1}$$

where $\boldsymbol{x} = (x,y,0)$ and $\boldsymbol{x}_s = (x_s,y_s,0)$ represent the source point and the observation point located on the traction-free surface, respectively. The function u_{ji}^* represents the *j-th* component of the displacement at point $\boldsymbol{x}$ due to a concentrated point force at point acting in the *i-th* direction and t_j represents the *j-th* component of the surface traction.

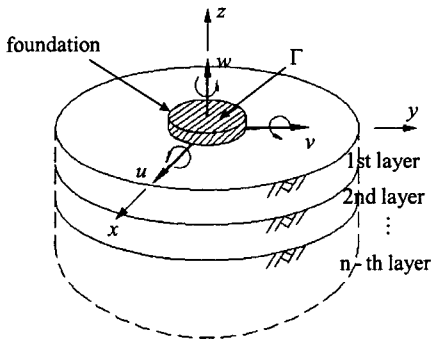

Figure 1 Surface structure on layered half-space

Since the horizontal flat surface is stress free, the traction of Green's functions automatically vanish on Γ. Using the quadratic shape function at each element, equation (1) is transformed into a system of linear algebraic equations

$$u_{ip}(\boldsymbol{x}) = \sum_{k=1}^{N} t_{jk} \left[\int_\Gamma u_{ji}^*(\boldsymbol{x}_s;\boldsymbol{x}) d\Gamma \right] \qquad (i,j = x,y,z) \tag{2}$$

with p, k = 1, 2, ..., N, where N is the total number of surface elements. The value u_{ip} represents the *i-th*

component of the displacement of the *p-th* element, and t_{jk} represents the *j-th* component of the surface traction in the *k-th* surface element. Equation (2) can be conveniently written in a matrix form as

$$\{u^{BE}\} = [G]\{t\} \tag{3}$$

where the matrix $[G]$, of dimension $3N \times 3N$, represents the force-displacement relationship between the elements of Γ and is called the compliance matrix for the flat surface Γ.

For the fundamental solutions, the receiver is assumed to be located in the *l-th* layer, the governing equations of motion in Cartesian coordinates can be obtained. Each layer is considered as homogeneous, isotropic and satisfies linearly elastic conditions. In the *l-th* medium, the transformed displacement field must satisfy the system of homogeneous or non-homogeneous ordinary second-order differential equations of motion. The displacement field due to point source in frequency domain can be summarized in the following form of equation:

$$u_{pq}^{\ell}(\omega, x) = \frac{1}{2\pi} \int_{-\infty}^{\infty} \left[\mathbf{D}_j^{\ell}(\omega, x; x_S) e^{-ikx^*} \right] dk \qquad p, q = x, y, z \tag{4}$$

where, i is $\sqrt{-1}$, p and q are the displacement and force direction, x^* is horizontal distance between source and receiver and h is source depth. k is the horizontal wavenumber and are the displacement $\mathbf{D}_j^{\ell}$ and stress vectors of P and SV waves with $z_u = z - z^{\ell-1}$, $z_d = z^{\ell} - z$.

Using the converging characteristics of displacement and stress vectors to the static solutions with increasing wavenumber k by Luco and Apsel(1983). The asymptotic solutions of Green's functions can be evaluated. Integrals of asymptotic solutions can be used out of the region *[-a,a]* in which the asymptotic solution accords with the numerical solution. Only within the region *[-a,a]*, numerical integration is used. The displacement vector and stress vector are presented as follows

$$u_{pq}^{l}(\omega, x) = \frac{1}{2\pi} \left[\int_{-a}^{+a} \{(\mathbf{D}_{nq}^{j}) e^{-ikx^*}\} dk + \int_{-\infty}^{a} \{(\tilde{\mathbf{D}}_{nq}^{j}) e^{-ikx^*}\} dk + \int_{+a}^{+\infty} \{(\tilde{\mathbf{D}}_{nq}^{j}) e^{-ikx^*}\} dk \right] \tag{5}$$

where n,p,q = x,y,z and $\mathbf{D}_{nq}^{j}$ is the displacement vector and stress vector of *j-th* layer, where subscript n is the direction of the displacement and q is the direction of the applied force, and k is the wave number of horizontal direction.

3. HYBRID FORMULATION FOR THE WAVE INPUTS

On the assumption that no slippage or uplift occurs at the soil-structure interface, the conditions of nodal forces equilibrium and nodal displacements compatibility can be used to match the two independently modeled substructures. For the total number of boundary elements used in the problem using shape function can be

written in the following form

$$\{u\}=\{u^{BE}\}=[N]\{u^{FE}\} \tag{6}$$

$$\{t\}=[N]\{P_r\} \tag{7}$$

where $\{u^{BE}\}$ and $\{t\}$ are the displacement vector and traction of boundary element. $\{u^{FE}\}$ and $\{P_r\}$ are displacement vector and nodal reaction force of finite element. In the modeling of structure, the plate element, which has five degrees of freedom at each node, is used. Therefore, the matrix $[N]$ is introduced to match the two different degrees of freedom. Considering the applied nodal force on the structure and displacement equilibrium requirements dictate that

$$P_{\text{int}} + P_r = P_{ext} \tag{8}$$

$$[\overline{K}]\{u\}+[N]^T[G]^{-1}[N]\{u\}=\{P_{ext}\} \tag{9}$$

where, $[\overline{K}]$ is modified stiffness of finite element. If equation (9) is arranged about the displacement vector $\{u\}$ as follows;

$$\{u\}=[[\overline{K}]+[N]^T[G]^{-1}[N]]^{-1}\{P_{ext}\}=[S]\{P_{ext}\} \tag{10}$$

Therefore, the relationship between external force and nodal displacement is established.

For the wave inputs, the total displacement and traction fields can be divided into two parts by Thau's suggestion(1967); the free field due to the incident wave waves, and the scattered field generated by the motion of the structure in the absence of any incident wave excitation. Also the traction fields can also be expressed in terms of nodal forces as

$$\{u_\tau\}=\{u_g\}+\{u_s\} \tag{11}$$

$$\{P_\tau\}=\{P_g\}+\{P_s\} \tag{12}$$

where $\{u_\tau\}$ and $\{P_\tau\}$ are the total displacement and nodal force vectors described at the nodes of the finite element discretization scheme, while the subscripts g and s indicate their free and scattered components, respectively. Recalling the relationship between external forces and their displacements, we obtain equation (13) combining with equation (3).

$$\{P_s\}=[G][\{u_\tau\}-\{u_g\}] \tag{13}$$

The equilibrium of nodal forces yields

$$\{P_{ext}\} = \{P_g\} + \{P_s\} + \{P_{\text{int}}\} \tag{14}$$

Where $\{P_{ext}\}$ is the total external force vector applied on the structure and $\{P_{\text{int}}\}$ is the internal elastic force vector of the structure substructure.

$$\{u_\tau\} = [S]^{-1}\left[[G]\{u_g\} - \{P_g\}\right] \tag{15}$$

Therefore the relationship between the unknown displacements at the soil-structure interface and the known incident wave excitation can be obtained after a direct substitution of equation (13) and (10) into equation (14), with $\{P_{\text{int}}\} = 0$ condition.

4. VERIFICATION OF FUNDAMENTAL SOLUTION

The following example demonstrates the validity of the developed fundamental solutions. Dynamic stiffness coefficients with resonance peaks due to a soil layer on a bedrock are computed, and the results are compared with the results of Luco(1974). The first layer is characterized by Young's modulus $E_1 = 1.76\times10^6 N/m^2$, Poisson's ratio $\nu_1 = 0.3$ and density $\rho_1 = 1.7\times10^3 kg/m^3$. The second layer, a bed rock, is characterized by Young's modulus $E_2 = 1.25\times10^7 N/m^2$, Poisson's ratio $\nu_2 = 0.25$ and density $\rho_2 = 2.0\times10^3 kg/m^3$. The above properties lead to a shear wave velocity ratio $RC_s = C_{s2}/C_{s1} = 2.5$. Also, the ratio of layer depth to radius(H/R) has constant number 0.5. *Figure* 2 shows the computed vertical stiffness coefficients normalized by the static stiffness. Here the frequency range is $0 \le a_0 \le 6$, with $a_0 = \omega R/C_{s1}$. The obtained results from this study closely agree with Luco's calculation results.

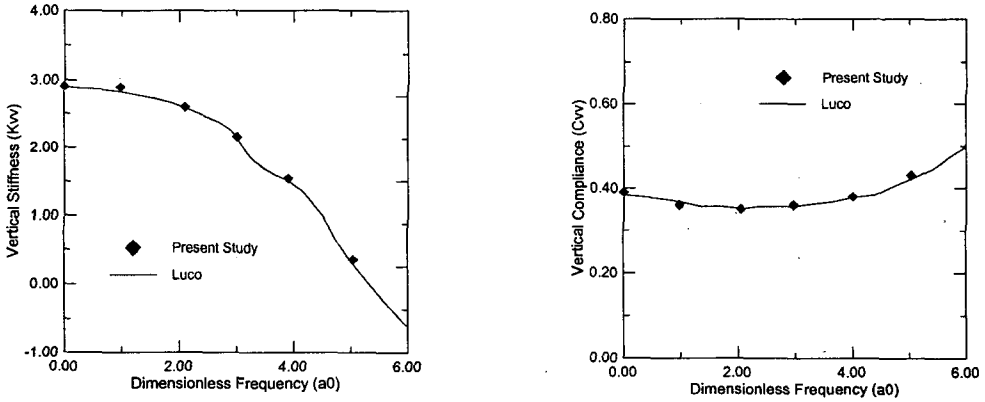

(a) Vertical stiffness (b) Vertical compliance

Figure 2 Response of surface structure on a layered half-space

5. INCIDENT WAVE RESPONSE OF CIRCULAR SURFACE STRUCTURE

The developed method is applied to the incident wave analysis of circular surface structure, shown in *Figure* 3. The dimensions of the structure are 7.3*m* for radius and 0.4*m* for thickness resting on the three layered half-space. The structure is discretized in sixteen quadratic elements with eighty-one nodal points. The thickness of first layer (H_1) is 5.0*m* and the second (H_2) is 10.0*m*. The properties of structure and layers are considered as variables to find the effects of those materials. Details of material properties are presented in Table 1.

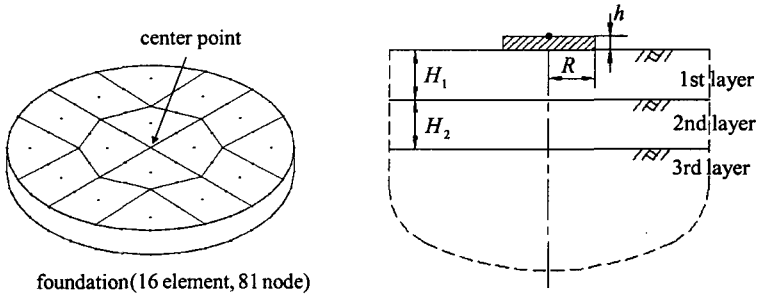

Figure 3 Structure on three layered half-space

The acceleration is the N-S component of *El-Centro* earthquake, was used as control motion on the ground surface. The peak ground acceleration(*PGA*) of the control motion is 0.319*g*. The control motion in time domain is transformed to that of frequency domain motion using FFT. The total time is

Table 1 Material properties of layered media

Layer \ Prop.	Young's Modulus (*Gpa*)		Density (kg/m^3)	Poisson's Ratio	Damping Ratio
1		0.5	1500	0.33	0.03
2	E_{S1}	0.8	1800	0.33	0.03
	E_{S2}	1.0			
	E_{S3}	2.0			
3		4.0	4000	0.33	0.03
Structure	E_{F1}	10.0	2300	0.33	0.01
	E_{F2}	20.0			
	E_{F3}	40.0			

20.46 seconds and upper limit of frequency is 25 *Hz*. The transformed incident wave loads are applied to the x-direction(100% of control motion) and z-direction(30% of control motion) for the horizontal and vertical motion. In *Figure* 4 and 5, the response of the center point on structure is represented in time history after the inverse FFT.

First, the horizontal displacements reduce significantly with increasing stiffness of structure as shown in *Figure* 4(a). Especially, in rigid structure(E_F = 500*Gpa*) the horizontal displacement converge to the input motion. Also, *Figure* 5(a) shows that the stiffness of second layer affects the response. In vertical case, descending trend of response is relatively small with increasing stiffness of structure and the second layer.

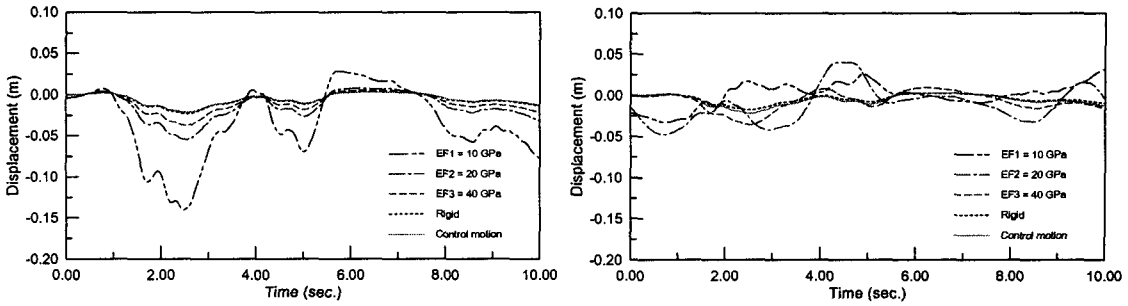

(a) Horizontal displacement (b) Vertical displacement

Figure 4 Displacement as variation of structure stiffness (E_S =1.0*Gpa*)

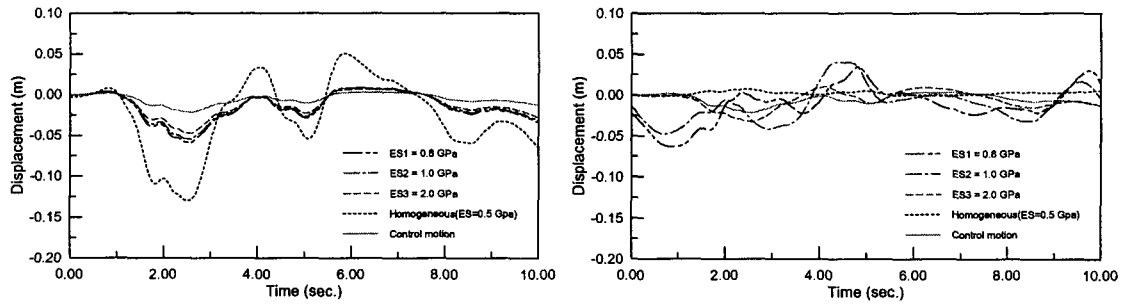

(a) Horizontal displacement (b) Vertical displacement

Figure 5 Displacement as variation of second layer stiffness (E_F =20*Gpa*)

However, the vertical response in the layered media is obviously different to the homogeneous case(*Figure* 5(b)). The layer effect occurs more apparently in vertical direction than in horizontal one. The reason is that the vertical wave experiences the reflection and defraction across the layers. Therefore, we can find that the layer effect of soil is an important in the vertical direction. In order to show briefly what is mentioned above, Figure 6 is introduced. In Figure 6 the perpendicular axis represents ratio of maximum displacement versus control motion and the horizontal axis normalizes the stiffness versus first case. The variation of stiffnesses of

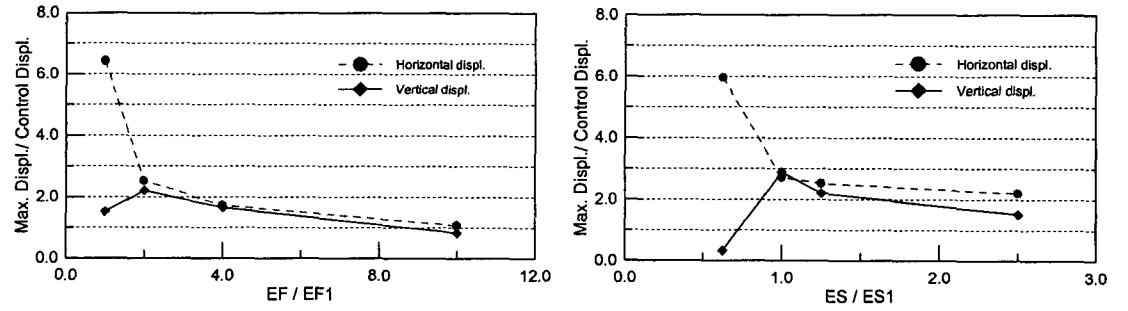

(a) As variation of structure stiffness (b) As variation of soil stiffness

Figure 6 Displacement as variation of second layer stiffness (E_F =20*Gpa*)

structure and soil layer is sufficient to control the maximum displacement in horizontal component but not in vertical case. It is caused by the layer effect of vertical displacement and the flexibility of structure.

6. CONCLUSIONS

Incident wave analysis of structures on layered half-space is performed in the frequency domain. The structures are modeled by finite elements and the layered half-space is modeled by boundary elements based on the fundamental solutions of the layered half-space using semi-analytical approach. For the incident wave input, the response is decomposed and formulated after the impedance matrix for the structure system. Numerical examples are presented to demonstrate the accuracy of the presented method.

As a result, it is shown that the stiffnesses of the sub-layer and structure are important factors to control the response of incident wave. The horizontal response reduces significantly as the stiffness of structure or layer increase. On the contrary, the vertical response change is not apparent. Thus, the increasing stiffness of structure may not be an effective way to lessen the vertical response. If the superstructure above the structure is critical to the vertical movement, the alternative way is needed to decrease the motion. Additionally, it is shown that the layer effect can be an important factor in soil-structure interaction problem.

ACKNOWLEDGEMENT

The partial support from Korea Gas Corporation R & D is gratefully acknowledged.

REFERENCES

1. Kim, M.K., Lim, Y.M. & Rhee, J.W.(1999). Dynamic responses of multi-layered half planes by coupled finite and boundary elements, *Engineering Structures*, (in printing).
2. Luco, J.E.(1974). Impedance functions for a rigid structure on a layered medium, *Nuclear Engineering and Design*, Vol.**31**, 204-217.
3. Luco, J.E. & Apsel, R.J.(1983). On the green's functions for a layered half-space, part I, *Bulletin of Seismological Society of America*, Vol.**73**, 909-929.
4. Mohammadi, M. & Karabalis, D.L.(1995). Dynamic 3-D soil railway track interaction by BEM-FEM, *Earthquake Engineering and Structural Dynamics*, Vol.**24**, 1177-1193.
5. Qian, J., Tham, L.G. & Cheung, Y.K.(1996). Dynamic cross-interaction between flexible surface footings by combined BEM and FEM, *Earthquake Engineering and Structural Dynamics*, Vol.**25**, 509-526.
6. Wong, H.L. & Luco, J.E.(1986). Dynamic interaction between rigid structures in layered half-space, *Soil Dynamics and Earthquake Engineering*, Vol.**5**, 149-158.